KYBERNETIKA — VOLUME *43* (2007), NUMBER 6, PAGES 841 – 854

DISLOCATION DYNAMICS – ANALYTICAL DESCRIPTION OF THE INTERACTION FORCE BETWEEN DIPOLAR LOOPS

Vojtěch Minárik and Jan Kratochvíl

The interaction between dislocation dipolar loops plays an important role in the computation of the dislocation dynamics. The analytical form of the interaction force between two loops derived in the present paper from Kroupa's formula of the stress field generated by a single dipolar loop allows for faster computation.

Keywords: dislocation dynamics, interaction force between dipolar loops

AMS Subject Classification: 35K65, 68U20, 74M25, 74S10

1. INTRODUCTION

A high density of edge dislocation dipolar loops is formed during plastic deformation of ductile materials [7, 8]. During deformation the loops are clustered becoming one of the main building blocks of the deformation microstructure which controls plastic, creep, fatigue, and fracture properties of these materials. The loops can be drifted by stress gradients and/or swept by glide dislocations and trapped by already existing clusters [1] to form dislocation patterns characteristic for various stages of the microstructure evolution.

The dislocation dynamics is a promising tool in modeling of microscopic mechanism of plasticity; however, the attempts to simulate the deformation substructure evolution involving dipolar loops have not yet been successful. The main reason is a large number of dipolar loops entering such simulation. As a consequence, one has to evaluate many particular interactions in each time step of the evolution. The more dipolar loops are incorporated in the computation, the more interactions one has to evaluate. For a particular dipolar loop in the model, there has to be evaluated its interaction with the glide dislocations as well as its interactions with all other dipolar loops. In such generality a simulation of the microstructure evolution is still a prohibitively complex problem.

Our particular model presented in [4, 5] has been focused on the detailed description of the motion of a number of dipolar loops interacting with a single glide dislocation. As has been documented in dislocation dynamics model [2] the mutual interactions among loops are vital in the process of their clustering; the loop interactions cannot be neglected in any simulations of dipolar loop pattering.

In this article, we present details of the analytical evaluation of the loop-to-loop interaction which is explored by the numerical algorithm DISDYN for simulation of dislocation dynamics described in [4, 5]. The formulae for the interaction forces between two loops of particular types and configurations (see [5]) are deduced from Kroupa's formula of the stress field generated by a single dipolar loop (see [3]).

2. GOVERNING EQUATIONS

The governing equations of the system of a single dislocation curve X and a number of dipolar loops of arbitrary types and configurations can be written as

$$B\dot{X} = \varepsilon X_{ss} + F X_s^{\perp} , \tag{1}$$

$$\frac{\mathrm{d}x^{(i)}(t)}{\mathrm{d}t} = \frac{1}{BP} F^{(i)}_{x,\mathrm{total}}(X, x^{(i)}(t)), \qquad i \in I \tag{2}$$

coupled with initial and boundary conditions.

Details of (1) describing the motion of the dislocation curve in 2D plane can be found in [4, 5], the model is being developed in correspondence with models of other phenomena in material structures, e. g. elastic behaviour (see [6]). We will focus on (2) describing the motion of the x-axis coordinate of the center of the ith dipolar loop – $x^{(i)}$. As B and P are constants (described elsewhere), the last remaining term in (2) is the total force $F^{(i)}_{x,\mathrm{total}}$ acting on the ith dipolar loop. This force includes interactions with all other dipolar loops as well as the interaction with the dislocation curve:

$$F^{(i)}_{x,\mathrm{total}} = \begin{cases} F_x^{c(i)} + F_x^{L(i)} - F_0 & \text{if} \quad F_x^{c(i)} + F_x^{L(i)} > F_0 , \\ 0 & \text{if} \quad |F_x^{c(i)} + F_x^{L(i)}| < F_0 , \\ F_x^{c(i)} + F_x^{L(i)} + F_0 & \text{if} \quad F_x^{c(i)} + F_x^{L(i)} < -F_0 . \end{cases}$$

The term $F_x^{c(i)}$ represents the interaction force between ith dipolar loop and the whole dislocation curve:

$$F_x^{c(i)} = \int_X \sigma^{(i)}_{xy} b_{\mathrm{curve}} n_x \, \mathrm{d}X , \tag{3}$$

where $\sigma^{(i)}_{xy}$ denotes the stress field generated by ith dipolar loop (therefore depending on the relative position of the dislocation curve's segment to the center of the ith dipolar loop). The term $F_x^{L(i)}$ covers all the interactions of ith dipolar loop with other dipolar loops:

$$F_x^{L(i)} = \sum_{j \neq i, j \in I} F(i,j) , \tag{4}$$

where $F(i,j)$ represents the interaction between the dipolar loops i and j and will be discussed later. Here we note $F(i,j)$ depends on types and configurations of both dipolar loops. Finally, F_0 is the lattice friction depending on material.

3. THE INTERACTION FORCE BETWEEN DIPOLAR LOOPS

For each time step in the numerical algorithm solving the system of a glide dislocation and the loops, we need to evaluate the interaction of each pair of dipolar loops present in the system. To allow faster computation, we derived analytical formulae for the interaction forces between two dipolar loops which can be summarized by the following theorem.

Theorem 3.1. Consider two dipolar loops in a stable configuration. Recalling the notation of previous papers[1], denote their types and configurations by V_1, V_2, I_1, or I_2, respectively[2]. Then, the interaction force between the two dipolar loops is given by one of the following formulae, depending on the combination of the types and configurations of both dipolar loops.

The first formula holds for the combinations $V_1 - V_2$, $V_1 - I_2$, $I_1 - V_2$, $I_1 - I_2$, $V_2 - V_1$, $V_2 - I_1$, $I_2 - V_1$, and $I_2 - I_1$:

$$\begin{aligned} F_x^{(1)} \;=\; & -\frac{\mu h^2}{\pi(1-\nu)} b'b'' \Bigg\{ \xi_1 \frac{-8x_0^5 + 64x_0^3y_0^2 - 24x_0y_0^4}{(x_0^2+y_0^2)^4} \\ & + \xi_{-1} \frac{-4x_0^5 + 32x_0^3y_0^2 - 12x_0y_0^4}{(x_0^2+y_0^2)^3} \\ & + \xi_{-3} \left((1-\nu)x_0 + \frac{-x_0^5 + 8x_0^3y_0^2 - 3x_0y_0^4}{(x_0^2+y_0^2)^2} \right) \\ & + \xi_{-5} \left(3x_0^3 \frac{-x_0^2+y_0^2}{x_0^2+y_0^2} \right) \Bigg\} . \end{aligned} \tag{5}$$

The second formula (using the upper signs) holds for the combinations $V_1 - V_1$, $V_1 - I_1$, $I_1 - V_1$, $I_1 - I_1$, and the third (with the lower signs) for $V_2 - V_2$, $V_2 - I_2$, $I_2 - V_2$, and $I_2 - I_2$:

$$\begin{aligned} F_x^{(2,3)} \;=\; & -\frac{\mu h^2}{\pi(1-\nu)} b'b'' \Bigg\{ -4\xi_1 \frac{x_0^5 \pm 9x_0^4y_0 - 2x_0^3y_0^2 \mp 14x_0^2y_0^3 - 3x_0y_0^4 \pm y_0^5}{(x_0^2+y_0^2)^4} \\ & + \xi_{-1} \frac{-2x_0^5 \mp 18x_0^4y_0 + 4x_0^3y_0^2 \pm 28x_0^2y_0^3 + 6x_0y_0^4 \mp 2y_0^5}{(x_0^2+y_0^2)^3} \\ & + \xi_{-3} \left((1+\nu)x_0 + \frac{-x_0^5 \mp 4x_0^4y_0 \pm 8x_0^2y_0^3 + x_0y_0^4}{(x_0^2+y_0^2)^2} \right) \\ & + \xi_{-5} \left(-3x_0^3 \frac{(x_0 \pm y_0)^2}{x_0^2+y_0^2} \right) \Bigg\} . \end{aligned} \tag{6}$$

[1] Each dipolar loop is one of the two types (vacancy or interstitial) and can exist in one of the two stable configurations, as described in details in [4, 5].

[2] Letters V and I stand for vacancy and interstitial dipolar loops, subindices 1 and 2 denote stable configurations

In the above formulae we use the following shorthand notation:

$$\begin{aligned}
\xi_1 &:= \rho_0(-2l) - 2\rho_0(0) + \rho_0(2l)\,, \\
\xi_{-1} &:= -\frac{1}{\rho_0(-2l)} + 2\frac{1}{\rho_0(0)} - \frac{1}{\rho_0(2l)}\,, \\
\xi_{-3} &:= -\frac{1}{\rho_0^3(-2l)} + 2\frac{1}{\rho_0^3(0)} - \frac{1}{\rho_0^3(2l)}\,, \\
\xi_{-5} &:= -\frac{1}{\rho_0^5(-2l)} + 2\frac{1}{\rho_0^5(0)} - \frac{1}{\rho_0^5(2l)}\,, \\
\rho_0(\omega) &:= \rho_0(x_0, y_0, z_0, \omega) := \sqrt{x_0^2 + y_0^2 + (z_0 + \omega)^2}\,.
\end{aligned}$$

Remarks 3.1.

3.1.1. We denote $[x_0, y_0, z_0]$ the mutual relative position of the centers of the dipolar loops, b' the x-axis component of the Burgers vector of the first dipolar loop, and b'' the x-axis component of the Burgers vector of the second dipolar loop. To close up the notation we have to add physical parameters, i. e. shear modulus μ, Poisson's ratio ν, the average half-width and half-length of a dipolar loop h and l.

3.1.2. It is enough to evaluate only the x-axis component of the interaction force (F_x) as the dipolar loops being of prismatic can move only along the Burgers vector which has in the present case the direction of the x-axis.

3.1.3. Although there is only one Burgers vector in the dislocation dynamics system, we explicitly use b' and b'' in the formulae because the sign can differ according to the type of the dipolar loop. This means, having Burgers vector of the modulus b, values of b' and b'' can be either $+b$ for a vacancy dipolar loop or $-b$ for an interstitial dipolar loop.

3.1.4. The second and the third formulae are very similar. This results from the fact the dipolar loops in the second and the third case are simply rotated by the angle of $\frac{\pi}{2}$. Therefore, one can easily prove that

$$F_x^{(2)}(x_0, y_0, z_0) = F_x^{(3)}(x_0, -y_0, z_0) \tag{7}$$

To prove the theorem we have to prepare following lemma.

Lemma 3.2. The total x-axis component of the force generated by a single dipolar loop positioned at the origin of the coordinate system and acting on a second dipolar loop positioned at $[x_0, y_0, z_0]$ is given by

$$\begin{aligned}
F_T^x &= 2hb\left(\sigma_{xz}(x_0, y_0, z_0 + l) - \sigma_{xz}(x_0, y_0, z_0 - l)\right) \\
&\quad + 2hb \int_{z_0 - l}^{z_0 + l} \left(\frac{\partial \sigma_{xy}(x_0, y_0, z)}{\partial y} \mp \frac{\partial \sigma_{xy}(x_0, y_0, z)}{\partial x}\, \mathrm{d}z \right)\,,
\end{aligned} \tag{8}$$

where σ_{xy} and σ_{xz} denote the components of the stress field tensor of the stress generated by the dipolar loop in the origin of the coordinate system. The upper sign in (8) holds for the dipolar loop of the type V_1, while the lower sign holds for the dipolar loop of the type V_2.

Remarks 3.2.

3.2.1. The only difference between V_1 and V_2 type of the dipolar loop in the formula (8) is in the sign before the term $\frac{\partial \sigma_{xy}}{\partial x}$.

3.2.2. If we need to evaluate the formula (8) for the I_1 or I_2 type of the dipolar loop, we only change the sign of b in the formula for the type V_1 or V_2, respectively.

P r o o f . To prove Lemma 3.2 let us first denote the vertices of the dipolar loop positioned at $[x_0, y_0, z_0]$. We will simultaneously prove the formula (8) for both configurations of the dipolar loop, i. e. V_1 and V_2.

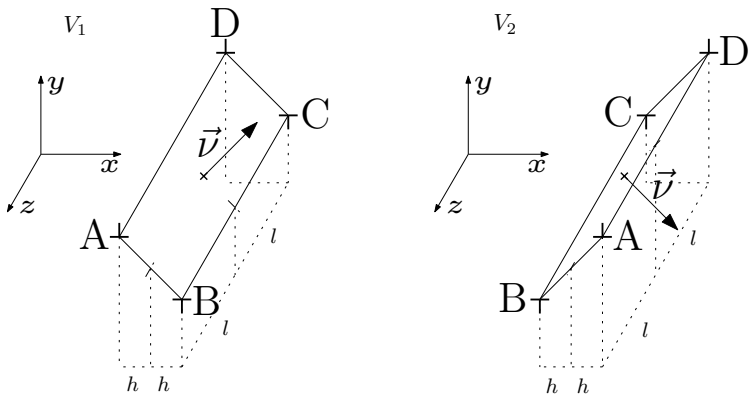

Fig. 1. Stable configurations V_1 and V_2 of dipolar loops positioned at $[x_0, y_0, z_0]$. The way of assigning letters A, B, C, and D to the vertices.

The following table summarizes the coordinates of the vertices:

configuration V_1		configuration V_2	
A	$[x_0 - h, y_0 + h, z_0 + l]$	A	$[x_0 + h, y_0 + h, z_0 + l]$
B	$[x_0 + h, y_0 - h, z_0 + l]$	B	$[x_0 - h, y_0 - h, z_0 + l]$
C	$[x_0 + h, y_0 - h, z_0 - l]$	C	$[x_0 - h, y_0 - h, z_0 - l]$
D	$[x_0 - h, y_0 + h, z_0 - l]$	D	$[x_0 + h, y_0 + h, z_0 - l]$

The interaction force per unit length of dislocation line is given by the Peach–Koehler equation, which written for the ith component reads

$$f_i = \varepsilon_{ijk}\sigma_{jm}b_m s_k \ , \tag{9}$$

where we denote:

- f_i — ith component of the interaction force per unit length of the dislocation line
- ε_{ijk} — Levi–Cività symbol
- σ_{jm} — components of the stress field tensor at the dislocation position
- b_m — components of the Burgers vector
- s_k — components of unit tangential vector of the dislocation line

To obtain F_T^x, we must integrate the Peach–Koehler equation along the dislocation lines of the dipolar loop positioned at $[x_0, y_0, z_0]$, i. e. along its shorter and longer sides.

Let us begin with the longer sides. Denote $\vec{s}$ the directional vector of the line DA, and $\vec{s'}$ the directional vector of the line BC:

$$\vec{s} = [0, 0, 1] \ , \quad \vec{s'} = [0, 0, -1] \ .$$

Denote the x-axis component of the interaction force per unit length of the dislocation line f^x and f'^x for the lines DA and BC, respectively:

$$f^x = f_1 = \varepsilon_{1j3}\sigma_{j1}b_1 s_3 = \varepsilon_{123}\sigma_{21}b_1 s_3 = b\sigma_{yx} = b\sigma_{xy} \ ,$$
$$f'^x = f_1' = \varepsilon_{1j3}\sigma_{j1}b_1 s_3' = \varepsilon_{123}\sigma_{21}b_1 s_3' = -b\sigma_{yx} = -b\sigma_{xy} \ .$$

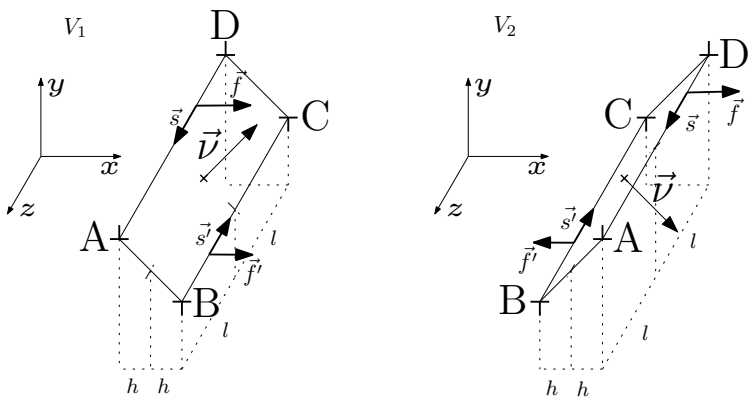

Fig. 2. Orientation of the tangential vectors $\vec{s}$ and $\vec{s'}$, and the x-axis components of the forces f and f' for the longer sides of dipolar loops.

The total force acting on the lines DA and BC is given by the integration of f^x and f'^x along the lines:

$$F^x = \int_{z_0-l}^{z_0+l} f^x \,\mathrm{d}z = b\int_{z_0-l}^{z_0+l} \sigma_{xy}(x_0 - h, y_0 + h, z)\,\mathrm{d}z \ ,$$
$$F'^x = \int_{z_0-l}^{z_0+l} f'^x \,\mathrm{d}z = -b\int_{z_0-l}^{z_0+l} \sigma_{xy}(x_0 + h, y_0 - h, z)\,\mathrm{d}z \ .$$

As we are interested in a total force acting on the whole dipolar loop, we sum F^x and F'^x together and obtain

$$F^x + F'^x = -2bh\int_{z_0-l}^{z_0+l} \left(\frac{\partial\sigma_{xy}(x_0, y_0, z)}{\partial x} - \frac{\partial\sigma_{xy}(x_0, y_0, z)}{\partial y}\right) \mathrm{d}z \ . \qquad (10)$$

The result in (10) was obtained using the Taylor expansion for σ_{xy} about the point $[x_0, y_0, z]$ and neglecting the terms containing h in the power of 2 or more. This can

be done under the assumption h is very small; it means that the derived expression is valid for distances between loops sufficiently larger than h:

$$\sigma_{xy}(x_0 - h, y_0 + h, z) \approx \sigma_{xy}(x_0, y_0, z) - h\frac{\partial\sigma_{xy}(x_0, y_0, z)}{\partial x} + h\frac{\partial\sigma_{xy}(x_0, y_0, z)}{\partial y} ,$$
$$\sigma_{xy}(x_0 + h, y_0 - h, z) \approx \sigma_{xy}(x_0, y_0, z) + h\frac{\partial\sigma_{xy}(x_0, y_0, z)}{\partial x} - h\frac{\partial\sigma_{xy}(x_0, y_0, z)}{\partial y} .$$

For the configuration V_2 we get the formula very similar to (10) which differs only in signs:

$$F^x + F'^x = 2bh\int_{z_0-l}^{z_0+l}\left(\frac{\partial\sigma_{xy}(x_0, y_0, z)}{\partial x} + \frac{\partial\sigma_{xy}(x_0, y_0, z)}{\partial y}\right)\mathrm{d}z. \tag{11}$$

For the shorter sides AB and CD the directional vectors $\vec{s}$ and $\vec{s'}$ depend on the configuration of the dipolar loop. For the configuration V_1 we have

$$\vec{s} = \left[\frac{1}{\sqrt{2}}, -\frac{1}{\sqrt{2}}, 0\right] , \quad \vec{s'} = \left[-\frac{1}{\sqrt{2}}, \frac{1}{\sqrt{2}}, 0\right] ,$$

while for the configuration V_2 it differs in signs:

$$\vec{s} = \left[-\frac{1}{\sqrt{2}}, -\frac{1}{\sqrt{2}}, 0\right] , \quad \vec{s'} = \left[\frac{1}{\sqrt{2}}, \frac{1}{\sqrt{2}}, 0\right] .$$

However, the x-axis components of the interaction forces per unit length of the dislocation line g^x and g'^x for the lines AB and CD, respectively, will be the same formulae for both configurations of the dipolar loop (due to the same y-axis component of the directional vector in both cases):

$$g^x = g_1 = \varepsilon_{1j2}\sigma_{j1}b_1 s_2 = \varepsilon_{132}\sigma_{31}b_1 s_2 = \frac{b}{\sqrt{2}}\sigma_{zx} = \frac{b}{\sqrt{2}}\sigma_{xz} ,$$
$$g'^x = g'_1 = \varepsilon_{1j2}\sigma_{j1}b_1 s'_2 = \varepsilon_{132}\sigma_{31}b_1 s'_2 = -\frac{b}{\sqrt{2}}\sigma_{zx} = -\frac{b}{\sqrt{2}}\sigma_{xz} .$$

The total force acting on the lines AB and CD is given by the integration of g^x and g'^x along the lines. For the configuration V_1 it reads[3]:

$$G^x = \sqrt{2}\int_{-h}^{h} g^x\,\mathrm{d}\eta = b\int_{-h}^{h}\sigma_{xz}(x_0 + \eta, y_0 - \eta, z_0 + l)\,\mathrm{d}\eta ,$$
$$G'^x = \sqrt{2}\int_{-h}^{h} g'^x\,\mathrm{d}\eta = -b\int_{-h}^{h}\sigma_{xz}(x_0 + \eta, y_0 - \eta, z_0 - l)\,\mathrm{d}\eta .$$

Similarly for the configuration V_2:

$$G^x = \sqrt{2}\int_{-h}^{h} g^x\,\mathrm{d}\eta = b\int_{-h}^{h}\sigma_{xz}(x_0 + \eta, y_0 + \eta, z_0 + l)\,\mathrm{d}\eta ,$$
$$G'^x = \sqrt{2}\int_{-h}^{h} g'^x\,\mathrm{d}\eta = -b\int_{-h}^{h}\sigma_{xz}(x_0 + \eta, y_0 + \eta, z_0 - l)\,\mathrm{d}\eta .$$

[3]The constant $\sqrt{2}$ in front of the integral comes from the substitution $\eta = \sqrt{2}\xi$ to make the integral bounds simpler to write

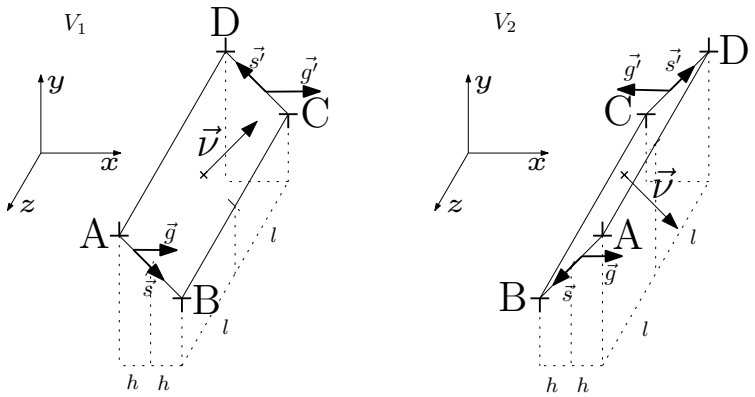

Fig. 3. Orientation of the tangential vectors $\vec{s}$ and $\vec{s}'$, and the x-axis components of the forces g and g' for the shorter sides of dipolar loops.

We assume h to be very small and use the Taylor expansions of σ_{xz} about the points $[x_0, y_0, z_0 + l]$ and $[x_0, y_0, z_0 - l]$ along the shorter sides of the dipolar loop. For the configuration V_1, arbitrary ζ, and η in the interval $[0, h]$ we get

$$\sigma_{xy}(x_0 - \eta, y_0 + \eta, \zeta) \approx \sigma_{xy}(x_0, y_0, \zeta) - \eta \frac{\partial \sigma_{xy}(x_0, y_0, \zeta)}{\partial x} + \eta \frac{\partial \sigma_{xy}(x_0, y_0, \zeta)}{\partial y} ,$$

$$\sigma_{xy}(x_0 + \eta, y_0 - \eta, \zeta) \approx \sigma_{xy}(x_0, y_0, \zeta) + \eta \frac{\partial \sigma_{xy}(x_0, y_0, \zeta)}{\partial x} - \eta \frac{\partial \sigma_{xy}(x_0, y_0, \zeta)}{\partial y} .$$

If we split the integral for G^x into two parts, it is obvious that all the partial derivatives vanish as the stress field is symmetric around the middle point $[x_0, y_0, z_0 + l]$ of the side AB:

$$\begin{aligned} G^x &= b \int_{-h}^{h} \sigma_{xz}(x_0 + \eta, y_0 + \eta, z_0 + l)\, \mathrm{d}\eta \\ &= b \int_{-h}^{0} \sigma_{xz}(x_0 + \eta, y_0 + \eta, z_0 + l)\, \mathrm{d}\eta + b \int_{0}^{h} \sigma_{xz}(x_0 + \eta, y_0 + \eta, z_0 + l)\, \mathrm{d}\eta \\ &= b \int_{-h}^{h} \sigma_{xz}(x_0, y_0, z_0 + l)\, \mathrm{d}\eta = 2hb\sigma_{xz}(x_0, y_0, z_0 + l) . \end{aligned}$$

Similarly, the partial derivatives in the formula for G'^x vanish too. As above for F^x and F'^x, we sum G^x and G'^x together and obtain

$$G^x + G'^x = 2bh\,(\sigma_{xz}(x_0, y_0, z_0 + l) - \sigma_{xz}(x_0, y_0, z_0 - l)) \tag{12}$$

for both configurations of the dipolar loop.

As the x-axis component of the total force acting on the dipolar loop positioned at $[x_0, y_0, z_0]$ is the sum along all the sides of the dipolar loop, the proof of the lemma is complete.

$$F_T^x = F^x + F'^x + G^x + G'^x \tag{13}$$

□

Before we begin the proof of Theorem 3.1, let us recall the stress field tensor formula presented by Kroupa et al [3] which uses Einstein's symbolic rule for sums over the indices $i, j, k, n \in \{1, 2, 3\}$:

$$\begin{aligned}\sigma_{ij} \quad = \quad & -\frac{\mu}{4\pi(1-\nu)} \iint\limits_A \frac{1}{\varrho^3} \left\{ \left[\frac{3(1-2\nu)}{\varrho^2} b_k \varrho_k \nu_n \varrho_n + (4\nu - 1) b_k \nu_k \right] \delta_{ij} \right. \\ & + (1-2\nu)\,(b_i \nu_j + b_j \nu_i) + \frac{3\nu}{\varrho^2} \left[b_k \varrho_k (\nu_i \varrho_j + \nu_j \varrho_i) + \nu_k \varrho_k (b_i \varrho_j + b_j \varrho_i) \right] \\ & \left. + \frac{3(1-2\nu)}{\varrho^2} b_k \nu_k \varrho_i \varrho_j - \frac{15}{\varrho^4} b_k \varrho_k \nu_n \varrho_n \varrho_i \varrho_j \right\} \mathrm{d}A \,.\end{aligned}$$

The symbols which were not yet introduced in this article follow:

A	area of the dipolar loop, with $\mathrm{d}A = 2h\sqrt{2}\,\mathrm{d}\zeta$
$\varrho_i, \varrho_j, \varrho_k, \varrho_n$	components of the relative position vector, $\varrho_1 = x, \varrho_2 = y, \varrho_3 = z$
ϱ	relative distance from the dipolar loop, $\varrho = \sqrt{\varrho_1^2 + \varrho_2^2 + \varrho_3^2}$
$\nu_i, \nu_j, \nu_k, \nu_n$	components of the dipolar loop normal vector
δ_{ij}	Kronecker symbol

P r o o f . The basic idea of the proof of Theorem 3.1 is to put Kroupa's formula of the stress field tensor into (8) and do as much analytical work as possible.

For h very small it is valid for the differential of dipolar loop's area that

$$\mathrm{d}A = 2h\sqrt{2}\,\mathrm{d}\zeta \,. \tag{14}$$

We rewrite the components of the stress field tensor that we need using (14). First, we consider σ_{xy}:

$$\begin{aligned}\sigma_{xy}(\varrho_1, \varrho_2, \varrho_3) \quad = \quad & \sigma_{12}(\varrho_1, \varrho_2, \varrho_3) = -\frac{\mu 2hb\sqrt{2}}{4\pi(1-\nu)} \int_{-l}^{l} \left\{ \frac{1}{\varrho^3} (1-2\nu)\,\nu_2 \right. \\ & + \frac{3\nu}{\varrho^5} \left[\varrho_1 (\nu_1 \varrho_2 + \nu_2 \varrho_1) + \varrho_2 (\nu_1 \varrho_1 + \nu_2 \varrho_2) \right] \\ & \left. + \frac{3(1-2\nu)}{\varrho^5} \nu_1 \varrho_1 \varrho_2 - \frac{15}{\varrho^7} \varrho_1^2 \varrho_2 (\nu_1 \varrho_1 + \nu_2 \varrho_2) \right\} \mathrm{d}\zeta \,.\end{aligned} \tag{15}$$

Now we replace ν_1 and ν_2 for the dipolar loop configuration[4] V_1 (the upper signs) or V_2 (the lower signs):

$$\begin{aligned}\sigma_{xy}(x, y, z) \quad = \quad & -\frac{\mu hb}{2\pi(1-\nu)} \int_{-l}^{l} \left\{ \pm (1-2\nu) \frac{1}{\varrho^3} \right. \\ & \left. + \left[\pm 3\nu \left(x^2 + y^2 \right) + 3xy \right] \frac{1}{\varrho^5} - 15\,(x \pm y)\, x^2 y \frac{1}{\varrho^7} \right\} \mathrm{d}\zeta \,.\end{aligned} \tag{16}$$

[4]Note we act here with the configuration of the loop positioned at the origin of the coordinate system

The only terms containing ζ in the integrand are the fractions of ϱ. These can be easily integrated. We skip this a little bit technical work and present the result:

$$\begin{aligned}\sigma_{xy}(x,y,z) &= -\frac{\mu h b}{2\pi(1-\nu)}\left\{\left[\frac{l-z}{\varrho_-}+\frac{l+z}{\varrho_+}\right]\left[\frac{x\pm y}{(x^2+y^2)^2}\left(\pm(x\pm y)-8\frac{x^2y}{x^2+y^2}\right)\right]\right.\\ &\quad+\left[\frac{l-z}{{\varrho_-}^3}+\frac{l+z}{{\varrho_+}^3}\right]\left[\pm\nu+\frac{xy}{(x^2+y^2)^2}\left(y^2-3x^2\mp 4xy\right)\right]\\ &\quad\left.+\left[\frac{l-z}{{\varrho_-}^5}+\frac{l+z}{{\varrho_+}^5}\right]\left[-\frac{3x^2y(x\pm y)}{x^2+y^2}\right]\right\}. \qquad (17)\end{aligned}$$

The component σ_{xz} will be processed similarly to σ_{xy}.

$$\begin{aligned}\sigma_{xz}(\varrho_1,\varrho_2,\varrho_3) &= \sigma_{13}(\varrho_1,\varrho_2,\varrho_3)\\ &= -\frac{\mu h b\sqrt{2}}{2\pi(1-\nu)}\int_{-l}^{l}\left\{\frac{3\nu}{\varrho^5}\left[\varrho_1\nu_1\varrho_3+(\nu_1\varrho_1+\nu_2\varrho_2)\,\varrho_3\right]\right.\\ &\quad\left.+\frac{3(1-2\nu)}{\varrho^5}\nu_1\varrho_1\varrho_3-\frac{15}{\varrho^7}\varrho_1^2\varrho_3\,(\nu_1\varrho_1+\nu_2\varrho_2)\right\}\mathrm{d}\zeta\end{aligned}$$

As before, we replace ν_1 and ν_2 for the dipolar loop configurations V_1 (upper signs) and V_2 (lower signs):

$$\begin{aligned}\sigma_{xz}(x,y,z) &= -\frac{\mu h b}{2\pi(1-\nu)}\int_{-l}^{l}\left\{\frac{3\nu}{\varrho^5}\left[x(z-\zeta)+(x\pm y)(z-\zeta)\right]\right. \qquad (18)\\ &\quad\left.+\frac{3(1-2\nu)}{\varrho^5}x(z-\zeta)-\frac{15}{\varrho^7}x^2(z-\zeta)(x\pm y)\right\}\mathrm{d}\zeta\\ &= -\frac{\mu h b}{2\pi(1-\nu)}\int_{-l}^{l}\left\{3(x\pm\nu y)\frac{z-\zeta}{\varrho^5}-15x^2(x\pm y)\frac{z-\zeta}{\varrho^7}\right\}\mathrm{d}\zeta\,.\end{aligned}$$

Recalling the definition of ϱ and its differential

$$\begin{aligned}\varrho(x,y,z-\zeta) &= \sqrt{x^2+y^2+(z-\zeta)^2}\\ \mathrm{d}\varrho &= \frac{z-\zeta}{\varrho}(-\mathrm{d}\zeta)\end{aligned}$$

it is easy to follow that the right-hand side of (18) is simple to integrate:

$$\begin{aligned}\int\frac{z-\zeta}{\varrho^5}\mathrm{d}\zeta &= -\int\frac{1}{\varrho^4}\frac{z-\zeta}{\varrho}(-\mathrm{d}\zeta)=-\int\frac{\mathrm{d}\varrho}{\varrho^4}=\frac{1}{3}\frac{1}{\varrho^3}\,,\\ \int\frac{z-\zeta}{\varrho^7}\mathrm{d}\zeta &= -\int\frac{1}{\varrho^6}\frac{z-\zeta}{\varrho}(-\mathrm{d}\zeta)=-\int\frac{\mathrm{d}\varrho}{\varrho^6}=\frac{1}{5}\frac{1}{\varrho^5}\,.\end{aligned}$$

Skipping the technical work we get to

$$\begin{aligned}\sigma_{xz}(x,y,z) &= -\frac{\mu h b}{2\pi(1-\nu)}\left\{\left[\frac{1}{{\varrho_-}^3}-\frac{1}{{\varrho_+}^3}\right](x\pm\nu y)\right. \qquad (19)\\ &\quad\left.-\left[\frac{1}{{\varrho_-}^5}-\frac{1}{{\varrho_+}^5}\right]\left(3x^2(x\pm y)\right)\right\}.\end{aligned}$$

Next, we need to get partial derivatives of (17) with respect to x and y and then integrate them in the formula (8). This is again only a highly technical process. Hence, it is possible to get exact analytical formulae for the partial derivatives of (17) as well as the resulting (8).

We must be careful here to avoid mixing Burgers vectors b between the dipolar loops (we should preserve the type of the stress generating dipolar loop — positioned at the origin of the coordinate system, and the type of the dipolar loop exposed to the generated stress).

Finally, we get to the 3 formulae of Theorem 3.1. □

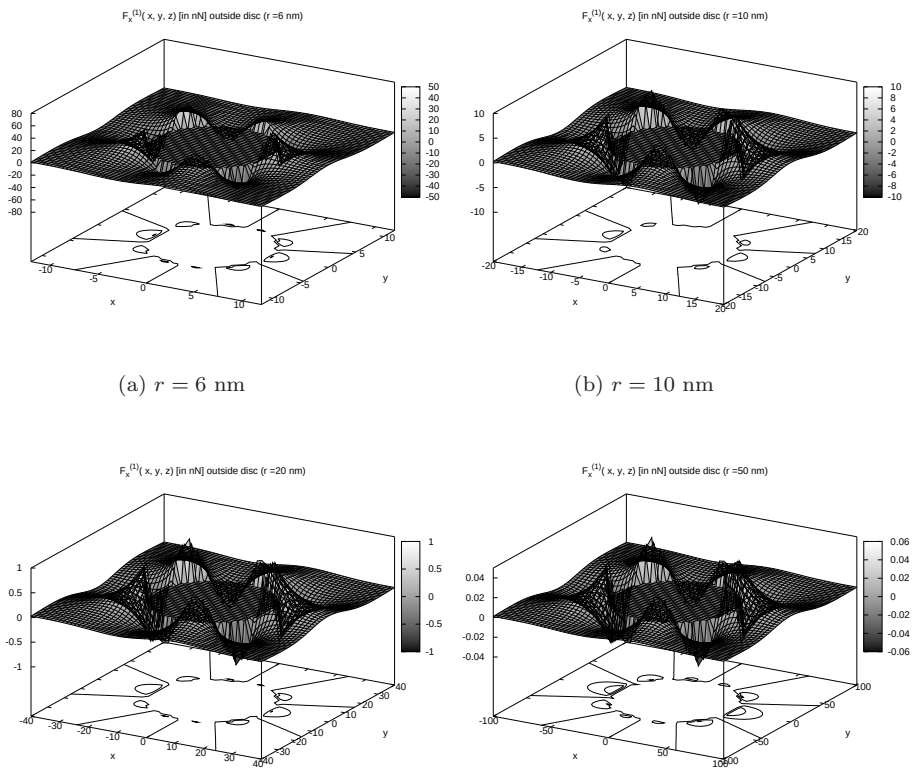

(a) $r = 6$ nm

(b) $r = 10$ nm

(c) $r = 20$ nm

(d) $r = 50$ nm

Fig. 4. Dependency of the force between two dipolar loops on the relative position of the centers of dipolar loops. For clearness, values in the central discs of growing radiuses around one of the dipolar loops are set to zero. This allows seeing the minimum and maximum values of the force beyond a circular threshold. Radiuses of the discs are 6, 10, 20, and 50 nm.

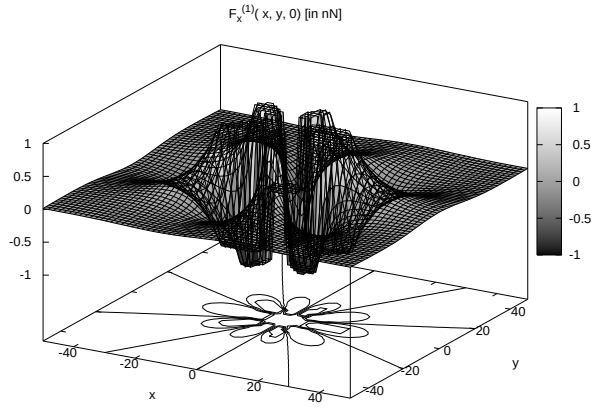

(e) Vacancy dipolar loops $V_1 - V_2$

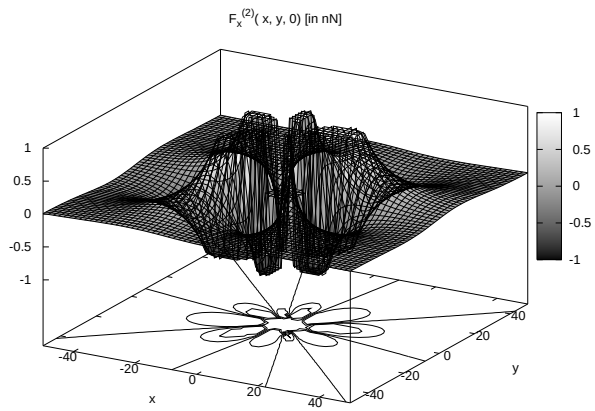

(f) Vacancy dipolar loops $V_1 - V_1$

Fig. 5. Force between two dipolar loops of different types and/or configurations placed in the same glide plane ($z = 0$): e) Vacancy dipolar loops of different configurations, f) Vacancy dipolar loops of the same configuration.

4. GRAPHS OF THE INTERACTION FORCE

In a dislocation dynamics simulation with a small density of dislocations, i. e. if the distances among dipolar loops are comparable with or greater than approximately

$3h$, we can use the above derived formulae to speed up the computation. However, if the density of dipolar loops is high and the distances among dipolar loops are smaller than $3h$, we get to the situation where the formulae are not accurate (because of the assumption of h small when comparing to the distance of the centers of the two dipolar loops in the proof of Theorem 3.1.

The real error of the interaction force formulae for very small distances of the two dipolar loops is still a matter of investigations. Therefore, the graphs of the interaction force between two dipolar loops presented here do not show the values for small distances ($\rho < 3h$).

Figure 5 shows the graphs of the force between two dipolar loops depending on the x and y relative position between the loops. The coordinate z is chosen to be 0. Two different combinations of types and configurations of the two dipolar loops are presented.

The force is very strong in the short range around the origin, i. e. around the position of one of the dipolar loops. It very rapidly looses its power with the increasing distance of the two dipolar loops.

To get the notion how fast the force interaction between two dipolar loops looses its power depending on the distance of the two dipolar loops, Figure 4 shows several graphs of the force $F_x^{(1)}(x, y, 0)$ with zero value discs of growing radiuses around the center of one of the dipolar loops. The minimal and maximal values of the interaction force outside the central discs can be easily read from the graphs.

ACKNOWLEDGEMENT

The first author was partly supported by the project No. MSM 6840770010 "Applied Mathematics in Technical and Physical Sciences", by the "Jindřich Nečas Center for Mathematical Modeling", project LC06052, and by the Czech–Slovak exchange project KONTAKT No. 83, all of the Ministry of Education, Youth and Sports of the Czech Republic, and by the NSF grant NSF00-138, Award 0113555. The second author was partly supported by the project KONTAKT No. ME654 and the grant VZ–MŠMT 6840770021. The conference participation was possible thanks to the Internal Grant of the Czech Technical University in Prague No. CTU 0617014.

(Received November 30, 2006.)

REFERENCES

[1] J. Bretschneider, C. Holste, and B. Tippelt: Cyclic plasticity of nickel single crystals at elevated temperatures. Acta Materialia *45* (1997), 3775–3783.

[2] J. Huang, N. M. Ghoniem, and J. Kratochvíl: On the sweeping mechanism of dipolar dislocation loops under fatigue conditions. Modelling and Simulation in Materials Science and Engineering *12* (2004), pp. 917–928.

[3] F. Kroupa: Long-range elastic field of semi-infinite dislocation dipole and of dislocation jog. Phys. Status Solidi *9* (1965), 27–32.

[4] V. Minárik, J. Kratochvíl, K. Mikula, and M. Beneš: Numerical simulation of dislocation dynamics. In: Numerical Mathematics and Advanced Applications, ENUMATH 2003 (peer reviewed proceedings) (M. Feistauer, V. Dolejší, P. Knobloch, K. Najzar, eds.), Springer–Verlag, Berlin 2004, pp. 631–641.

[5] V. Minárik, J. Kratochvíl, and K. Mikula: Numerical simulation of dislocation dynamics by means of parametric approach. In: Proc. Czech Japanese Seminar in Applied Mathematics (M. Beneš, J. Mikyška, and T. Oberhuber, eds.), Faculty of Nuclear Sciences and Physical Engineering, Czech Technical University in Prague 2005, pp. 128–138.
[6] T. Oberhuber: Numerical solution for the Willmore flow of graphs, In: Proc. Czech Japanese Seminar in Applied Mathematics 2005 (M. Beneš, M. Kimura and T. Nakaki, eds.), COE Lecture Note Vol. 3, Faculty of Mathematics, Kyushu University Fukuoka 2006, pp. 126–138
[7] B. Tippelt: Influence of temperature on microstructural parameters of cyclically deformed nickel single crystals. Philos. Mag. Letters *74* (1996), 3, 161–166.
[8] B. Tippelt, J. Bretschneider, and P. Hähner: The dislocation microstructure of cyclically deformed nickel single crystals at different temperatures. Phys. Status Solidi (A) *163* (1997), 11–26.

Vojtěch Minárik, Department of Mathematics, Faculty of Nuclear Sciences and Physical Engineering, Czech Technical University in Prague, Trojanova 13, 120 00 Praha 2. Czech Republic.
e-mail: minarikv@kmlinux.fjfi.cvut.cz

Jan Kratochvíl, Department of Physics, Faculty of Civil Engineering, Czech Technical University in Prague, Thákurova 7, 166 29 Praha 6. Czech Republic.
e-mail: kratochvil@fsv.cvut.cz